

LUMINOSITY FUNCTIONS, RELATIVISTIC BEAMING, AND UNIFIED THEORIES OF HIGH-LUMINOSITY RADIO SOURCES

P. PADOVANI

European Southern Observatory, Karl-Schwarzschild-Str. 2, D-8046 Garching bei München, F.R.G.

AND

C. M. URRY

Space Telescope Science Institute, 3700 San Martin Drive, Baltimore, MD 21218

Received 1991 June 5; accepted 1991 September 16

ABSTRACT

If relativistically beamed emission dominates the observed radio flux from flat-spectrum radio quasars, as suggested by their rapid variability, polarization, and superluminal motion, then there must be counterpart sources whose emission is beamed at larger angles to the line of sight. We evaluate such unified schemes quantitatively, with steep-spectrum radio quasars and high-luminosity radio galaxies constituting the misaligned sources. Our procedure compares the number densities and luminosities of the separate populations, taking into account the strong selection effects introduced by relativistic beaming.

First, we derive the local luminosity functions of high-luminosity (i.e., Fanaroff-Riley type II) radio galaxies, flat-spectrum quasars, and steep-spectrum quasars. Then we calculate the luminosity functions predicted by a relativistic beaming model and compare them to the observed ones. We find very good agreement both for flat- and steep-spectrum quasars for a distribution of Lorentz factors $5 \lesssim \gamma \lesssim 40$ (skewed toward lower values) that was estimated from the observed distribution of superluminal speeds for flat-spectrum quasars. Our model predicts that flat-spectrum quasars have their radio axes within $\theta \sim 14^\circ$ of the line of sight, steep-spectrum quasars are in the range $14^\circ \lesssim \theta \lesssim 40^\circ$, and high-luminosity radio galaxies occupy the remaining angles. The alternative hypothesis that flat-spectrum quasars are simply the beamed version of steep-spectrum ones, with Fanaroff-Riley type II radio galaxies belonging to a separate class, does not give as good a fit to the data.

Subject headings: galaxies: jets — galaxies: nuclei — galaxies: fundamental parameters — radio continuum: galaxies

1. INTRODUCTION

The possibility that radio emission from extragalactic sources is relativistically beamed has been considered for the past quarter-century. Relativistic bulk motion in radio-emitting plasmas can explain the apparent superluminal motion revealed by VLBI observations (reviews by Porcas 1987; Cohen 1989; Zensus 1989), the one-sidedness of the core-jet morphology in radio quasars on both small (parsec) and large (kiloparsec) scales (Cawthorne 1991; Bridle & Perley 1984), and the unphysically high brightness temperatures (Quirrenbach et al. 1989) and lack of self-Compton X-rays (Marscher et al. 1979) in compact variable radio sources. Indeed, relativistic beaming easily accounts for the coupling of high luminosities with the rapid variability, high polarization, and compact morphologies that define blazar-like sources.

The real test of the relativistic beaming hypothesis rests on its predictions for whole classes of active galactic nuclei (AGNs). Because of the enormous flux enhancement caused by relativistic aberration, orientation effects would grossly distort the classification system. Unification schemes represent an attempt to identify as intrinsically the same those objects whose perceived characteristics differ only because of orientation bias. If the “parent population” consists of the objects with misaligned beaming axes and “beamed” objects are those whose relativistic motion is oriented more closely along the line of sight, then the numbers and luminosities of the beamed

and parent populations must correspond in the way predicted by the simple consequences of relativistic beaming.

Orientation biases other than relativistic beaming, such as inherently anisotropic emission (e.g., from a thick accretion disk) or obscuration of an isotropic source (e.g., by a dusty torus), are not considered here because the full range of flux enhancement in these cases is very small compared to relativistic beaming and is generally important only for near-infrared through soft X-ray emission.

Unification of different classes of AGNs has been considered a number of times over the past decade or so. Arguably the most successful unification scheme to date is the association of BL Lac objects with low-luminosity radio galaxies. The recognition that the characteristics of BL Lac objects implied relativistically beamed emission was first pointed out by Blandford & Rees (1978), and recent evidence of the ubiquity of superluminal motion in BL Lac objects (Mutel 1990; Urry, Padovani, & Stickel 1991) certainly bears this out. The most likely parent population, based on unbeamed characteristics like large-scale radio structure, host galaxy type, and emission-line properties, consists of the Fanaroff-Riley type I (F-R I) radio galaxies (Wardle, Moore, & Angel 1984; Antonucci & Ulvestad 1985; Ulrich 1989). Estimates of the relative numbers and luminosities of the two classes, based either on unbeamed properties or incorporating some corrections for the selection biases introduced by beaming, confirmed the plausibility of

this identification (Browne 1983; Schwartz & Ku 1983; Browne 1989), although the samples involved were small and/or incomplete.

There are always two choices in calculations of unification schemes: either focusing on unbeamed properties or trying to take selection effects into account. Although the former method is adequate for estimating population statistics, it is worrisome that the strong selection effects due to beaming have already occurred in the sample selection. With the relatively shallow samples now available, this can be a serious limitation.

A detailed prescription for incorporating selection biases into consideration of flux-limited samples was discussed by Urry & Shafer (1984) and extended by Urry & Padovani (1991). This formalism describes the predicted luminosity function of beamed objects given the luminosity function of the parent population. The application of this method to BL Lac objects and F-R I galaxies, using sizable and complete X-ray and radio samples, as well as the less complete optical data available, quantified the proposed unification scheme and constrained some details of the beaming model (Padovani & Urry 1990, 1991; Urry et al. 1991).

There are many similarities between BL Lac objects and flat-spectrum radio quasars (FSRQs). In particular, their continua are similar in shape, in polarization, and in variability. The idea that all quasars are relativistically beamed is supported by recent studies suggesting that most, if not all, FSRQs are highly polarized and rapidly variable, i.e., blazar-like (Fugmann 1988; Impey & Tapia 1990). Moreover, superluminal motion is common in FSRQs, more so than in steep-spectrum radio quasars (SSRQs; Hough & Readhead 1989). Although the relationship between F-R I (low-luminosity) and F-R II (high-luminosity) radio galaxies is unclear, as is the relationship between weak-lined (BL Lac objects) and strong-lined (FSRQs) blazars, it is plausible that by analogy the F-R II radio galaxies might contain relativistically beamed cores, and therefore might have some blazar-like daughter population aligned with the line of sight. We therefore consider unification schemes for radio galaxies and quasars under the assumption that relativistically beamed radio emission causes the observed distinction between them.

Scheuer & Readhead (1979) proposed the first unification scheme involving quasars, specifically, that radio-quiet quasars could form the parent population of radio-loud quasars. This picture was later ruled out because of differences in the strength of the large-scale, diffuse, unbeamed emission between the two classes. In a still viable scenario, Orr & Browne (1982) suggested that SSRQs might form the parent population of FSRQs. This was supported by the shape of the 2.7 GHz counts of FSRQs that were predicted from the SSRQ counts; however, this model still has not been stringently tested due to incomplete information about the space distribution and evolution of these classes (e.g., Peacock 1987). A more recent suggestion, discussed by Peacock (1987) and explored by Barthel (1989), is that the parent population of all radio quasars consists of radio galaxies, with FSRQs the most aligned and SSRQs at intermediate angles to the line of sight. The linear size distributions of radio-galaxies and quasars (mostly SSRQs since Barthel used the low-frequency-selected 3C RR sample) support this hypothesis. Differences in the optical line emission properties were explained by invoking cylindrical obscuration with the same axis as the beamed radio emission.

This hypothesis has not been tested quantitatively incorporating the effects of beaming. Barthel (1989) tested this hypoth-

esis using the 3C RR survey, which because of its low selection frequency (178 MHz) may represent "unbeamed" and therefore unbiased selection; however, it has only two flat-spectrum objects and so Barthel tested only the connection between radio galaxies and SSRQs. Peacock (1987) did discuss the Orr & Brown (1982) SSRQs/FSRQs hypothesis by calculating a correction for relativistic beaming and comparing luminosity functions. However, his flat-spectrum sources included BL Lac objects, and the total number density of flat-spectrum sources he derived was larger than the number density of SSRQs! He also mentioned the possibility of F-R II galaxies as the parent population, but did not do the related calculation. With the additional redshift information now available, it is possible to determine separate luminosity functions and evolutionary behavior for FSRQs, SSRQs, and F-R II galaxies, and to test the full beaming hypothesis quantitatively in terms of population statistics.

In this paper we use the most recent available information to calculate for the first time the luminosity functions and evolutionary behavior of all three classes. Previous determinations of the luminosity functions generally divided radio samples into steep-spectrum sources (mixing galaxies and quasars) and flat-spectrum sources (mixing quasars and BL Lac objects). Next, we use the formalism of Urry & Shafer (1984) and Urry & Padovani (1991) to make a model-dependent prediction of the luminosity functions of SSRQs and FSRQs assuming they represent increasing alignment along the line of sight and that F-R II galaxies are the parent population. In this picture the intrinsic Lorentz factors in all three classes must be the same, although the apparent values derived from superluminal data will be different because of orientation effects. By comparing predicted and observed quasar luminosity functions we are able to constrain the details of the relativistic beaming of radio emission.

In § 2 we describe the radio flux-limited sample used and the classification of the radio sources. In § 3 we study the evolutionary properties and derive the luminosity functions of F-R II galaxies, SSRQs and FSRQs. In § 4 we calculate the predicted radio luminosity function for FSRQs under the beaming hypothesis, which depends primarily on the Lorentz factor(s) characterizing the radio-emitting region. VLBI observations of FSRQs suggest that there is a distribution of intrinsic Lorentz factors. Assuming a simple form for this distribution, we find the predicted luminosity function that best agrees with the data. In § 5 a similar procedure is used to compare the predicted radio luminosity function for SSRQs to the observed one, although at this point the distribution of Lorentz factors is fixed. In § 6 we discuss our results and evaluate remaining uncertainties. Finally, the conclusions are summarized in § 7. Throughout this paper the values $H_0 = 50 \text{ km s}^{-1} \text{ Mpc}^{-1}$ and $q_0 = 0$ have been used unless stated otherwise.

2. A RADIO FLUX-LIMITED SAMPLE OF GALAXIES AND QUASARS

There are two primary requirements for the radio flux-limited sample of galaxies and quasars to be used. First, the selection frequency must be high enough that the sample is not biased against flat-spectrum sources. Second, optical identifications and redshifts must be available for a large fraction of the sample so that reliable luminosity functions can be constructed. The best sample available is then the 2 Jy sample (Wall & Peacock 1985), a complete flux-limited sample selected at 2.7 GHz, covering 9.81 sr, and including 233 sources with $F_{2.7} \geq 2 \text{ Jy}$. We have updated the redshifts and optical identifi-

cations using the latest version of the 1 Jy catalog (Stickel & Kühr 1992); all sources but three F-R II galaxies in the 2 Jy catalog are also in the 1 Jy catalog (Kühr et al. 1981).

The 2 Jy catalog contains the following classes of objects, as described in Table 1.

1. *Fanaroff-Riley type I galaxies*: galaxies with a radio brightness peaked around the optical counterpart (Fanaroff & Riley 1974). Thirty-six galaxies are so classified in the literature, and we include five more with $P_{2.7} < 1.6 \times 10^{32}$ ergs $s^{-1} Hz^{-1}$, the minimum power for F-R II galaxies in the 3C RR catalog. All these objects have measured redshifts.

2. *Fanaroff-Riley type II galaxies*: galaxies with radio emission brightest at the ends of the radio lobes. Twenty-nine galaxies have this morphological classification in the literature, eight more are classified as uncertain F-R II galaxies, and for 46 we could not find any classification. Only 17 of the galaxies with uncertain or no classification have $P_{2.7} < 5.8 \times 10^{33}$ ergs $s^{-1} Hz^{-1}$, the maximum power for F-R I galaxies in the 3C RR catalog, and are therefore possible F-R I galaxies. However, since the fraction of certain F-R I galaxies in the power range $1.6 \times 10^{32} < P_{2.7} < 5.8 \times 10^{33}$ ergs $s^{-1} Hz^{-1}$ (i.e., the region of overlap between the two classes) is 28% in the 2 Jy sample, similar to the fraction of F-R I galaxies in the same power range in the 3C RR, the uncertain and unclassified galaxies in this interval are probably all F-R II galaxies and were so considered. Twenty-six sources (i.e., 31% of the class) have uncertain redshifts, i.e., redshifts estimated from V magnitudes by Wall & Peacock.

3. *Compact galaxies*: galaxies whose radio brightness distribution is dominated by an unresolved component. Only two galaxies have this morphological classification.

4. *Steep-spectrum radio quasars*: quasars with spectral index $\alpha > 0.5$ ($F \propto \nu^{-\alpha}$) between 2.7 and 5 GHz. Five objects in this group were classified as Seyfert 1 galaxies by Véron-Cetty & Véron (1989) and as N galaxies by Spinrad et al. (1985). All the objects in this class have measured redshifts.

5. *BL Lacertae objects*: sources with flat radio spectral indices ($\alpha \leq 0.5$ between 2.7 and 5 GHz) and optical spectra without strong emission lines (rest-frame equivalent widths less than 5 Å). All seven BL Lac objects in the 2 Jy sample also belong to the 1 Jy sample of Stickel et al. (1991). One of these has an uncertain redshift.

6. *Flat-spectrum radio quasars*: quasars with spectral index $\alpha \leq 0.5$ between 2.7 and 5 GHz that were not classified as BL Lac objects by Stickel et al. (1991). Following the discussion in the Introduction, we have included in this class CTA 102 even though it has $\alpha = 0.67$ in Wall & Peacock (1985; but $\alpha = 0.5$ in Kühr et al. 1981) because it has high optical polarization

($p > 3\%$; Impey & Tapia 1990), it is a superluminal source (Zensus 1989), and it is core-dominated (Browne & Murphy 1987). All the FSRQs have measured redshifts.

7. *Empty Fields (EF)*: radio sources with no (or contradictory) optical identifications. This includes 12 steep-spectrum and four flat-spectrum sources that were either specified as empty fields or classified as G? or Q? by Wall & Peacock (1985) and for which no further identification was found. These unidentified sources constitute a small fraction of the total sample and should not affect our results.

The division between steep- and flat-spectrum sources at a spectral index $\alpha = 0.5$ is admittedly an arbitrary convention (its significance depending also on the simultaneity of the flux measurements). Nevertheless, it appears to separate sources quite well according to the dominance of the synchrotron emission and evidence of relativistic bulk motion. In fact, 58% of flat-spectrum sources in the 2 Jy sample; i.e., all the BL Lac objects and half the FSRQs have optical polarization $p_{\max} > 3\%$, while of the 13 SSRQs with polarization data only one (3C 390.3) has $p_{\max} > 3\%$ (Impey & Tapia 1990; Impey, Lawrence, & Tapia 1991). At least 28% of flat-spectrum sources are superluminal (see § 4.1), i.e., 43% of the BL Lac objects and 26% of the FSRQs (basically all of those observed with VLBI), while only two SSRQs (3C 245 and 3C 390.3) display superluminal motions. Finally, flat-spectrum sources are core-dominated, while SSRQs are lobe-dominated (see §§ 4 and 5).

The numbers of objects in each class and their mean radio spectral indices and mean redshifts are given in Table 1. Note that the supposed parent and beamed populations do not have similar redshift distributions. The beamed objects have in fact higher luminosities on average and in a flux-limited sample will therefore be visible at higher redshifts. The mean redshifts reported in Table 1 are therefore consistent with the beaming hypothesis (compare FR-I galaxies and BL Lac objects, and F-R II galaxies, SSRQs, and FSRQs).

The biggest problem of the 2 Jy sample for our purposes is the large fraction (nearly one-third) of F-R II galaxies with uncertain redshift estimates, which will seriously affect the reliability of the F-R II luminosity function. Another concern is the fact that the evolutionary properties of F-R II galaxies in the 2 Jy sample differ from those of radio galaxies in other samples (see § 3). To derive the luminosity function of F-R II galaxies we therefore chose to use the sample of F-R II galaxies from the 3C RR catalog (Laing, Riley, & Longair 1983), which includes 173 radio sources, all with morphological identification, having $F_{178\text{ MHz}} \geq 10$ Jy and covering 4.05 sr (galactic latitude $|b^{\text{II}}| \geq 10^\circ$ and declination $\delta \geq 10^\circ$). The optical identification of the catalog is basically complete (e.g., Spinrad et al.

TABLE 1
PROPERTIES OF THE RADIO SAMPLE

Class	N	$\langle \alpha_{2.7}^2 \rangle$	$\langle z \rangle$	Uncertain or no z
F-R I galaxies	41	0.79 ± 0.04^a	0.035 ± 0.006	...
F-R II galaxies	83	0.82 ± 0.03	0.34 ± 0.04	31%
Compact galaxies	2	0.82 ± 0.21	0.40 ± 0.35	...
SSRQs	34	0.81 ± 0.03	0.72 ± 0.09	...
BL Lacs	7	0.14 ± 0.09	0.38 ± 0.12	14%
FSRQs	50	-0.09 ± 0.06	1.15 ± 0.10	...
SS EF or no ID	12	0.93 ± 0.06	...	100%
FS EF or no ID	4	0.29 ± 0.09	...	100%
F-R II galaxies (3C RR)	91	0.94 ± 0.02	0.58 ± 0.05	...

^a Excluding NGC 1275 ($\alpha_{2.7}^2 = -2.58$) and 3C 120 ($\alpha_{2.7}^2 = -1.71$).

1985; Djorgovski et al 1988); it contains 91 F-R II galaxies, all with measured redshifts (see Table 1). Fluxes at 2.7 GHz and spectral indices between 2.7 and 5 GHz were derived from Wall & Peacock (1985) and Kellermann, Pauliny-Toth, & Williams (1969) for all but two objects, for which the 2.7 GHz fluxes were estimated from the flux at 178 MHz and the spectral index between 178 and 750 MHz.

We note that all but three of the 2 Jy sources would have been detected in the 3C RR had the surveyed areas been the same, as estimated from their fluxes and spectral indices. The 3C RR is, in fact, slightly deeper than the 2 Jy catalog, with $\sim \frac{2}{3}$ of the sources having $F_{2.7} < 2$ Jy and a minimum flux of $F_{2.7} \simeq 0.5$ Jy. This difference between the two catalogs should not affect our results (see next section).

3. EVOLUTION AND LUMINOSITY FUNCTIONS

Strong radio sources are known to evolve considerably, as first shown by Schmidt (1968), and therefore their luminosity functions will depend on redshift. However, the number of objects per class is still too small to study the evolving luminosity functions directly (the statistics per redshift bin would be too poor). The simplest way to make full use of the data is to estimate the evolution for each class and then to de-evolve the objects accordingly and derive the local luminosity functions.

The study of evolutionary properties can be addressed through the V/V_m test (Schmidt 1968), where V is the volume enclosed by an object and V_m is the maximum accessible volume within which it could have been detected above the flux limit of the sample. In the absence of evolution the quantity V/V_m has the property of being uniformly distributed between 0 and 1, with a mean value of 0.5 (Schmidt 1968).

We calculated the values of V/V_m for F-R II galaxies, SSRQs, and FSRQs, using the comoving volume appropriate for a Friedmann-Robertson-Walker cosmology and taking into account the K -correction by using the individual spectral slopes. The mean values for the different classes are given in Table 2.

As mentioned in the previous section, the 2 Jy F-R II galaxies do not show strong evolution, with $\langle V/V_m \rangle = 0.57 \pm 0.03$, consistent with no evolution at the $\sim 2 \sigma$ level. This differs from the behavior of F-R II galaxies in the 3C RR sample, which have $\langle V/V_m \rangle = 0.65 \pm 0.03$. Quasars and 3C RR (F-R II) radio galaxies show comparable evolution at the $3\text{--}5 \sigma$ level with $\langle V/V_m \rangle \sim 0.65$, an already established result (e.g., Laing et al. 1983).

Particular evolutionary models can be fitted to the observed values of $\langle V/V_m \rangle$. We considered luminosity evolution of the form $P(z) = P(0) \exp[-T(z)/\tau]$, where $T(z)$ is the look-back time and τ is the time scale of evolution in units of the Hubble time. The best-fit evolution parameter τ is the value that makes $\langle V/V_m \rangle$ equal to 0.5, and the goodness of fit is then given by the uniformity of the distribution of the V/V_m once the effect of evolution has been taken into account. (This method was used,

for example, by Maccacaro et al. 1983 to quantify the evolution of X-ray-selected AGNs.) The 1σ interval of τ corresponds to the values for which $\langle V/V_m \rangle = 0.5 \pm 1/(12N)^{1/2}$, where N is the number of objects in the sample (Longair & Scheuer 1970).

The best-fit evolution parameters are reported in Table 2, which shows that the values for the different classes are consistent within $1\text{--}1.5 \sigma$. In each case the distribution of V/V_m , corrected for evolution, is consistent with being uniform between 0 and 1 according to a Kolmogorov-Smirnov (K-S) test, implying that the exponential evolution model describes the data adequately. The values of τ for the different classes are in very good agreement with those derived by Danese et al. (1987) for high-luminosity radio sources, i.e., $\tau \simeq 0.24$ and $\tau \simeq 0.19$ for flat- and steep-spectrum sources, respectively. Dunlop & Peacock (1990) found a decline of the luminosity functions of radio sources in the redshift range $z \sim 2\text{--}4$, which is obviously inconsistent with a pure luminosity evolution continuing to those redshifts. This does not affect our results, however, since only about 5% of the sources have $z > 2$ and none has a redshift larger than 3.

Using the derived values for the evolution parameter, we computed the zero redshift luminosity at 2.7 GHz, $P_{2.7}(0) = P_{2.7}(z) \exp[-T(z)/\tau]$, for each object. We then calculated the local luminosity functions using Schmidt's (1968) estimator $\sum 1/V_m$, where V_m takes into account the effects of evolution. The resulting local luminosity functions are shown in Figure 1, with error bars representing the 1σ Poisson errors (Gehrels 1986).

A few interesting features can be noted in the figure. First, there is an increase in luminosity going from F-R II galaxies to steep-spectrum quasars to flat-spectrum quasars: the mean luminosities derived from the luminosity functions are $\langle P_{2.7} \rangle \simeq 4 \times 10^{32}$, 9×10^{32} , and 7×10^{33} ergs s^{-1} Hz $^{-1}$, respectively. Second, the luminosity functions of SSRQs and F-R II galaxies are similar in shape over the common range of powers, up to $P_{2.7} \sim 10^{34}$ ergs s^{-1} Hz $^{-1}$, but the SSRQs are lower in number density by a factor ~ 3 . The ratio of the number densities of the two classes for $P_{2.7} \gtrsim 5 \times 10^{32}$ ergs s^{-1} Hz $^{-1}$ is 3.1, in good agreement with the factor of 2.5 Barthel (1989) found by simply dividing the number of 3C RR

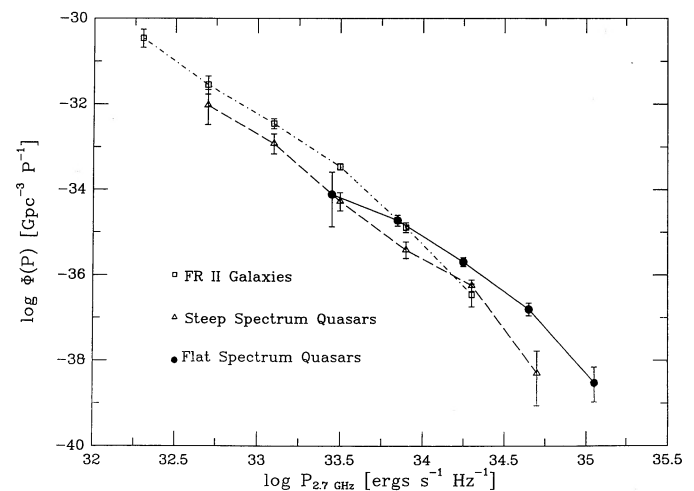


FIG. 1.—Local luminosity functions for radio sources: filled circles represent flat-spectrum radio quasars, open triangles represent steep-spectrum radio quasars, while open squares represent F-R II galaxies. The error bars indicate 1σ errors assuming Poisson statistics (Gehrels 1986).

TABLE 2

EVOLUTIONARY PROPERTIES OF DIFFERENT CLASSES

Class	$\langle V/V_m \rangle$	τ
F-R II galaxies (2 Jy)	0.57 ± 0.03	$0.28^{+0.20}_{-0.07}$
F-R II galaxies (3 CR)	0.65 ± 0.03	$0.17^{+0.03}_{-0.02}$
SSRQs	0.64 ± 0.05	$0.16^{+0.06}_{-0.03}$
FSRQs	0.64 ± 0.04	$0.23^{+0.07}_{-0.04}$

galaxies and quasars in the redshift range 0.5–1. Third, FSRQs become the dominant population for $P_{2.7} > 10^{34}$ ergs s⁻¹ Hz⁻¹ and their luminosity function flattens toward lower luminosities.

The F-R II luminosity function derived from the 2 Jy sample agrees well with the one derived from the 3C RR sample at low luminosities (in particular the minimum luminosity, an important parameter for the beaming model, is the same) but is flatter at high luminosities, as expected from the smaller relative evolution (i.e., larger τ). We checked that using the 3C RR sample, selected at 178 MHz instead of 2.7 GHz, does not bias our results. First, the luminosity function of 3C RR F-R II galaxies derived assuming a value of the evolutionary parameter appropriate for the 2 Jy F-R II galaxies (i.e., $\tau \approx 0.28$) is indistinguishable from the luminosity function of the latter. Second, if we restrict ourselves to the 3C RR F-R II galaxies having $F_{2.7} \geq 2$ Jy (about $\frac{1}{3}$ of the sample), the corresponding luminosity function is consistent with the one of the whole sample of 3C RR F-R II galaxies. This shows that neither the different selection frequency nor the different flux limits affect the resulting luminosity function very much.

It is interesting to note that the properties of the FSRQs do not seem to depend strongly on the degree of optical polarization. Both low-polarization quasar (LPQ) and high-polarization quasar (HPQ) subclasses have similar average spectral indices, $\langle V/V_m \rangle$, and τ . The redshift distributions differ at the 98% confidence level (K-S test), in the sense that HPQs seem to have on average smaller redshifts than LPQs, but this may be a selection effect due to the decrease in polarization with decreasing rest wavelength (Wills 1989). The luminosity functions seem to be slightly different as well, with the low-polarization objects having a lower space density. This could reflect the duty cycle of polarization if all FSRQs are intrinsically identical. Due to the relatively small numbers of objects involved, however, these comparisons need to be redone with larger samples.

4. THE LUMINOSITY FUNCTION OF FSRQs: BEAMING PREDICTIONS VERSUS OBSERVATIONS

4.1. Method of Calculation

According to the beaming hypothesis, FSRQs are F-R II galaxies with jets aligned with the line of sight. Under a set of simple assumptions—primarily that all jets are unidirectional and randomly oriented with respect to the line of sight, and that the intrinsic jet luminosity is related to the unbeamed luminosity in a straightforward way—the luminosity function of the beamed (aligned) objects can be derived directly from the luminosity function of the parent population. In this paper we follow the method and notation of Urry & Shafer (1984), and Urry & Padovani (1991). Briefly, the observed luminosity, L_j , of a relativistic jet is related to its emitted luminosity, \mathcal{L}_j , via $L_j = \delta^p \mathcal{L}_j$, where δ , the kinematic Doppler factor for the jet, is defined by $\delta = [\gamma(1 - \beta \cos \theta)]^{-1}$, β is the velocity in units of the speed of light, $\gamma = (1 - \beta^2)^{-1/2}$ is the Lorentz factor, and θ is the angle between the velocity vector and the line of sight. The value of p depends on the shape of the emitted spectrum and on the detailed physics of the jet (e.g., Lind & Blandford 1985). In the following we take $p = 3 + \alpha$ but a possible different choice will be discussed in § 6.

We consider a two-component model in which the total luminosity of a source L_T , is the sum of an unbeamed part \mathcal{L}_u and a jet luminosity $L_j = \delta^p \mathcal{L}_j$. Then if the intrinsic jet lumi-

nosity is proportional to the unbeamed luminosity, $\mathcal{L}_j = f \mathcal{L}_u$, the total luminosity is $L_T = \mathcal{L}_u + L_j = (1 + f\delta^p) \mathcal{L}_u$. We define as beamed those sources which have a ratio between observed jet luminosity and unbeamed luminosity $R \equiv L_j / \mathcal{L}_u = f\delta^p$, larger than some value R_{\min} . The largest angle between the jet and the line of sight for beamed objects is a critical angle, θ_c , defined by the condition $R_{\min} \equiv f\delta_{\min}^p$, where $\delta_{\min} = \delta(\theta_c)$. Similarly, the largest ratio, $R_{\max} \equiv f\delta_{\max}^p$, will occur at the smallest angle, θ_{\min} (usually $\theta_{\min} = 0$).

Urry & Shafer (1984) showed that for the simplest case of a single Lorentz factor and a parent luminosity function represented by a power law with index B and sharp cutoffs at \mathcal{L}_1 and \mathcal{L}_2 , the beamed luminosity function is a double power law, of index B above the break luminosity and index $(p + 1)/p$ below the break (if $B > [p + 1]/p$). This result has recently been extended by Urry & Padovani (1991) to include more general parent luminosity functions, especially those with more gradual low-luminosity cutoffs, and to allow a distribution of Lorentz factors rather than a single value.

In this formalism, the “parent population” really means all intrinsically identical objects regardless of orientation—in this case, F-R II galaxies plus SSRQs plus FSRQs. When Doppler boosting is strong so that beaming is an important effect, the radiation cone is small and the number of beamed objects relative to the parents is small. In that case the distinction between the luminosity function of parents and of parents-minus-beamed-objects can be ignored. Under the present hypothesis, however, the SSRQs are not very strongly beamed, and indeed F-R II galaxies are only a factor of 3 more numerous than SSRQs. Therefore we use as the parent luminosity function the F-R II luminosity function multiplied by the factor 1.3.

The radio luminosity function of F-R II galaxies derived in § 2 is not well represented by a single power law ($\chi^2_\nu \approx 3.4$ for 4 degrees of freedom). However, it can be fitted very well by two power laws ($\chi^2_\nu \approx 0.08$ for 2 degrees of freedom), breaking at $P_{2.7} \approx 10^{33.6 \pm 0.2}$ ergs s⁻¹ Hz⁻¹, with slopes $B_1 = 2.48 \pm 0.15$ and $B_2 = 3.9 \pm 0.7$, below and above the break, respectively. The total number density of F-R II galaxies (for $P_{2.7} \gtrsim 1.3 \times 10^{32}$ ergs s⁻¹ Hz⁻¹) is ≈ 81 Gpc⁻³. We will show in the next section that a distribution of Lorentz factors is suggested by superluminal motion data for FSRQs. Therefore, we calculate the predicted beamed luminosity function of FSRQs for the case of a jet plus isotropic emission, double power-law parent luminosity function, and a distribution in γ (described in § 4 of Urry & Padovani 1991; see also Urry et al. 1991).

4.2. Superluminal Motion and the Distribution of Lorentz Factors

If superluminal motion is an illusion resulting from bulk relativistic motion, then the *minimum* Lorentz factor responsible for the observed superluminal velocity is $\gamma_{\min} = (1 + \beta_{\text{app}}^2)^{1/2}$ (Pearson & Zensus 1987). An ensemble of jets with the same bulk speed and a range of angles to the line of sight from 0 to $> 1/\gamma$ will have an observed distribution of Lorentz factors up to the true Lorentz factor, with smaller observed values corresponding to larger angles to the line of sight or to closely aligned vectors ($\theta < 1/\gamma$). The distribution of observed Lorentz factors therefore contains information about the true value (or distribution of values) of the jet Lorentz factor(s).

VLBI observations of 13 FSRQs in the 2 Jy sample are available in the literature (Zensus 1989; Wehrle, Cohen, & Unwin 1990). For these, proper motion data were transformed

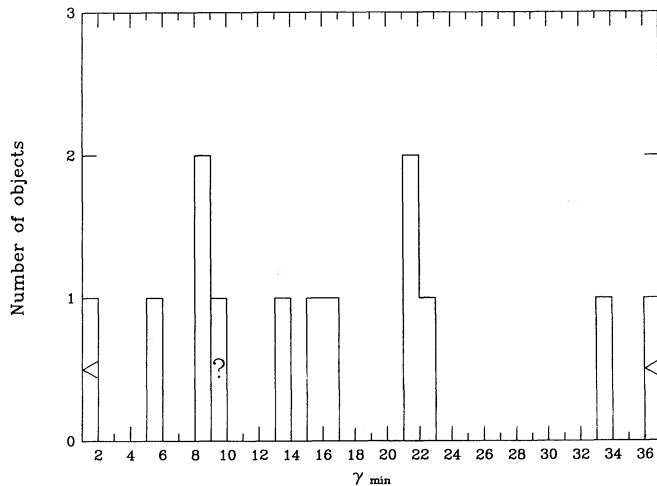


FIG. 2.—The distribution of superluminal Lorentz factors $\gamma_{\min} = (1 + \beta_{\text{app}}^2)^{1/2}$ for the 2 Jy sample of flat-spectrum radio quasars. The values of β_{app} have been derived from the proper-motion data assuming $H_0 = 50 \text{ km s}^{-1} \text{ Mpc}^{-1}$ and $q_0 = 0$. Lower and upper limits are indicated accordingly, while a question mark indicates uncertain values.

to apparent velocities, $\beta_{\text{app}} = v_{\text{app}}/c$, using the cosmology adopted in this paper ($H_0 = 50 \text{ km s}^{-1} \text{ Mpc}^{-1}$, $q_0 = 0$). Every one of the 13 FSRQs shows evidence of superluminal motion ($\beta_{\text{app}} > 1$); the distribution of γ_{\min} for the fastest component of each is shown in Figure 2. The values of γ_{\min} for other FSRQs not in the 2 Jy sample lie in a similar range (5–30).

The average γ_{\min} is ~ 17 , but the distribution is very broad. If a single value of the Lorentz factor were responsible for the observed distribution of apparent velocities, it would have to be larger than ~ 35 , the largest value of γ_{\min} ; however, in that case the distribution would be strongly peaked toward the high end (Cohen 1989), contrary to what is observed. The superluminal data, while sparse, therefore suggest a distribution of Lorentz factors extending to at least $\gamma \sim 35$ and probably skewed toward low values.

According to the beaming hypothesis, SSRQs and F-R II galaxies have the same intrinsic distribution of jet velocities, but because the viewing angles are relatively large, the measured values should be smaller, as indeed is the case for the few SSRQs with superluminal data (see § 5).

4.3. Predicted versus Observed Luminosity Function

The luminosity function predicted by the beaming model depends on the parent luminosity function, derived in § 4.1; the value of $p = 3 + \alpha \simeq 2.9$, since the mean value of the radio spectral index of FSRQs is $\alpha \simeq -0.1$; and the values of f and γ , which can be constrained by the observed values of R_{\min} and R_{\max} .

Estimates for the ratio of core to extended emission were found in literature for about $\frac{3}{4}$ of FSRQs (Browne & Perley 1986; Browne & Murphy 1987; Wills & Browne 1986; Hough & Readhead 1987; Antonucci & Ulvestad 1985; Antonucci et al. 1986) and were converted to 2.7 GHz rest frequency taking $\alpha_{\text{extended}} - \alpha_{\text{compact}} = 1$. The range of ratios runs from $R_{\min} \simeq 0.3$ to $R_{\max} \simeq 1550$. (The distribution of R is incomplete, but see the discussion for the effect of a larger range on our results in § 6.1.) Since a distribution of Lorentz factors is suggested by the VLBI data (see previous section), the beamed luminosity function will depend on the assumed distribution function and range of γ . For simplicity we assume a power-law distribution

of Lorentz factors, which is in fact fairly general (see Urry & Padovani 1991). In order to keep the number of free parameters at a minimum, the lower value was fixed to $\gamma_1 = 5$, since only one FSRQ has $\gamma_{\min} < 5$ (see Fig. 2), and the upper value was fixed to $\gamma_2 = 40$, since superluminal motion data can give only a lower limit to the Lorentz factor. We are then left with just one free parameter, the slope G of the distribution function $n(\gamma) \propto \gamma^G$. We note that the value of f is fixed by R_{\max} and γ_2 : $f = R_{\max}/[\gamma_2(1 + \beta_2)]^p \simeq 4.5 \times 10^{-3}$.

With these parameters we calculate from the luminosity function of the parents the luminosity function predicted for FSRQs, to be compared directly with the observed one derived in § 3. It has to be noted that the observed luminosity function is quite sensitive to the exact value of the evolution parameter τ , especially at high luminosities. Therefore, the error bars for the various bins have been derived by summing in quadrature the Poisson errors and the variations of the luminosity function associated with a 1σ change in τ . Apart from the first two bins, which are almost independent of τ , the latter dominate, being typically a factor of ~ 3 larger than the former.

Figure 3 shows the comparison between observations and the predictions of the beaming model. The best-fit predicted luminosity function ($\chi^2_{\nu} \simeq 0.41$ for 4 degrees of freedom) was derived for a Lorentz factor distribution with $G \simeq -2.3$, which implies $\langle \gamma \rangle \simeq 11$. The 1σ interval for G , derived for values of $\chi^2 = \chi^2_{\min} + 1$ (Lampton, Margon, & Bowyer 1976), is $[-3.7, -1.1]$. Taking into account the simplifying assumptions in the model and the fact that there was only one free parameter, the agreement is impressive. The total number density of FSRQs (above $P_{2.7} \simeq 1.7 \times 10^{32} \text{ ergs s}^{-1} \text{ Hz}^{-1}$) is predicted to be $N_{\text{FSRQ}} \simeq 2.2 \text{ Gpc}^{-3}$, or 2% of the parents. The predicted number counts and redshift distribution agree well with the observed ones, as must be the case because they are uniquely determined by the luminosity function, evolution, and cosmology.

The critical angles for the extreme values of γ —that is, the angle between the jet and the line of sight within which the object looks like a FSRQ (see eq. [A4] of Padovani & Urry

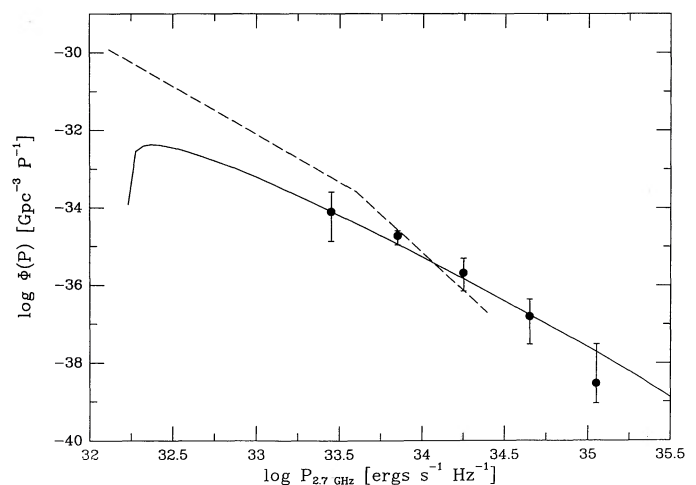


FIG. 3.—The differential luminosity function of FSRQs (solid line) as predicted by the beaming model compared to the observational estimates (filled circles). The differential luminosity function of F-R II galaxies (dashed line) is also shown. The error bars have been derived by summing in quadrature the Poisson errors (Gehrels 1986) and the variations of the number density associated with a 1σ change in the evolutionary parameter τ .

1990)—are $\theta_c(\gamma_1) \simeq 13.5^\circ$ and $\theta_c(\gamma_2) \simeq 6.1^\circ$. That is, FSRQs should be found for $\theta \lesssim 14^\circ$.

5. THE LUMINOSITY FUNCTION OF SSRQs: BEAMING PREDICTIONS VERSUS OBSERVATIONS

According to the beaming hypothesis, the SSRQs are supposed to be at intermediate angles, but their intrinsic properties—in particular, the value(s) of γ —must be identical to those of the FSRQs. Therefore, with these parameters already fixed, we can compare the predicted luminosity function of SSRQs to the observed one.

The method of calculation is similar to the one used in the previous section; however, since SSRQs are supposed to be misaligned objects, $\theta_{\min} \neq 0$. Assuming there is no overlap between the two classes, we take $\theta_{\min} = 13.5^\circ$, the largest value of the critical angle for FSRQs.

The formalism of Urry & Shafer (1984) and Urry & Padovani (1991) can easily accommodate $\theta_{\min} \neq 0$. The main change is that, while for $\theta_{\min} = 0$, $R_{\max} \equiv f\delta(0, \gamma_2)$, now $R_{\max} \equiv f\delta[\theta_{\min}, \gamma'(\theta_{\min})]$, where γ' can assume any value between γ_1 and γ_2 , depending on θ_{\min} . As a result, for a given value of R_{\max} , f is normally larger and the beamed luminosity function is more similar to the parent one. As expected, in the limit of large θ_{\min} , the two luminosity functions become indistinguishable, independent of the value of the Lorentz factor.

In this case $p = 3 + \alpha \simeq 3.8$, since the mean value of the radio spectral index of SSRQs is $\alpha \simeq 0.8$. Estimates for the ratio of core to extended emission were found in literature for about half the SSRQs (Browne & Murphy 1987; Wills & Browne 1986). They were converted to 2.7 GHz rest frequency as described in the previous section, deriving then $R_{\min} \simeq 0.01$ and $R_{\max} \simeq 1.7$. In the beaming hypothesis the intrinsic value(s) of the Lorentz factor have to be the same for FSRQs and SSRQs. Therefore, we assume a distribution of Lorentz factors $n(\gamma) \propto \gamma^{-2.3}$ for $5 \leq \gamma \leq 40$, as derived for FSRQs. Note that in this case we have no free parameters. As before, the error bars for the various bins have been derived by summing in quadrature the Poisson errors and the variations of the luminosity function associated with a 1σ change in τ . Again, apart from the first two bins which are almost independent of τ , the latter dominate, being typically a factor of ~ 3 larger than the former.

Figure 4 shows the comparison between observations and the predictions of the beaming model. The agreement is quite good ($\chi^2_\nu \simeq 1.1$ for 6 degrees of freedom). The value of f is $\simeq 7 \times 10^{-3}$, only a factor of 1.5 larger than the one derived for FSRQs. The critical angles for the extreme values of γ are $\theta_c(\gamma_1) \simeq 38^\circ$ and $\theta_c(\gamma_2) \simeq 14^\circ$. The fit could easily be improved by adjusting the model parameters. For example, if we take $n(\gamma) \propto \gamma^{-3.5}$, consistent within 1σ with the best fit for the FSRQs, then $\chi^2_\nu \simeq 0.7$. Similarly, while the predicted number counts and redshift distribution are consistent with the observed ones, the fit could be improved by finding the best compromise parameter for FSRQs and SSRQs simultaneously. The important point is, however, that the same distribution of Lorentz factors produces a good fit to both the luminosity function of FSRQs and SSRQs.

Note that the model-dependent value of $\simeq 38^\circ$ we find for the angle separating SSRQs from F-R II galaxies is in very good agreement with the angle derived from the number density ratio found in § 3, $\theta = \arccos(1 + 1/3.1)^{-1} \simeq 41^\circ$. We remind the reader that the latter estimate is valid only when

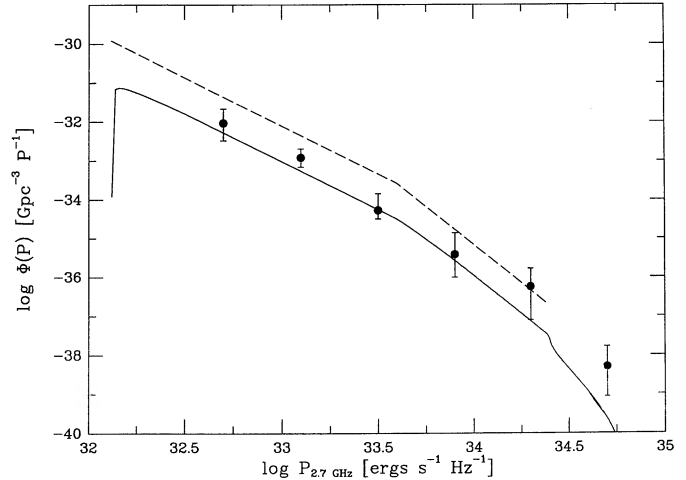


FIG. 4.—The differential luminosity function of SSRQs (solid line) as predicted by the beaming model compared to the observational estimates (filled circles). The differential luminosity function of F-R II galaxies (dashed line) is also shown. The error bars have been derived by summing in quadrature the Poisson errors (Gehrels 1986) and the variations of the number density associated with a 1σ change in the evolutionary parameter τ .

dealing with unbeamed luminosities or when the effect of beaming is not very strong because the objects are viewed off-axis, as in this case.

6. DISCUSSION

In the previous sections we have shown that the hypothesis that both flat- and steep-spectrum radio quasars are beamed F-R II galaxies, at increasing angles to the line of sight, is consistent with the observed properties of these classes. In particular, the luminosity functions have the right shape and normalization, providing that intrinsically the jets have approximately 1% of the unbeamed luminosity, and that there is a range of Lorentz factors between ~ 5 and ~ 40 , with $\langle \gamma \rangle \sim 11$. These parameters were estimated from the observed distribution of superluminal Lorentz factors of FSRQs, and by matching the observed and predicted luminosity functions of FSRQs. The independent calculation for SSRQs agrees very well with observations. This provides strong support for the hypothesis that relativistic beaming of the radio emission is the main cause of the apparent differences between radio galaxies and quasars.

6.1. Dependence of Results on Input Parameters

Our results, and the derived distribution of Lorentz factors, depend on a number of observational parameters which are inevitably uncertain. It is therefore important to test the stability of the agreement between predictions and observations, showing also how the inferred parameters change for plausible different input values.

1. γ_1, γ_2 .—The extreme values of the Lorentz factors are uncertain. The range of Lorentz factors could easily be larger than assumed, since only about $\frac{1}{4}$ of FSRQs have VLBI data. If we take $\gamma_1 = 3$ and $\gamma_2 = 45$ both the FSRQ and SSRQ observed luminosity functions are consistent with the predicted ones for $n(\gamma) \propto \gamma^{-1.4}$: $\chi^2_\nu \simeq 1$ for 4 degrees of freedom and $\chi^2_\nu \simeq 1$ for 5 degrees of freedom is in fact obtained for FSRQs and SSRQs, respectively. The details of the distribution change, but the mean value of the Lorentz factor (now $\langle \gamma \rangle \simeq 12$) changes little.

2. R_{\max} , R_{\min} .—Data for the ratio of core to extended emission are available for the majority of the objects; however, the range of values could be larger than the observed one. Taking $R_{\max} = 5000$ for the FSRQs and $n(\gamma) \propto \gamma^{-4}$ i.e., $\langle \gamma \rangle \simeq 7.4$, we get $\chi_v^2 \simeq 1.6$ for 4 degrees of freedom for the FSRQs and $\chi_v^2 \simeq 0.7$ for 5 degrees of freedom for the SSRQs. If we take $R_{\min} = 0.1$ for the FSRQs, keeping the other parameters unchanged, we obtain $\chi_v^2 \simeq 0.4$ for 4 degrees of freedom for the FSRQs and $\chi_v^2 \simeq 0.9$ for 5 degrees of freedom for the SSRQs. Taking $R_{\max} = 10$ for the SSRQs, we get $\chi_v^2 \simeq 0.6$ for 5 degrees of freedom, while if $R_{\min} = 0.003$ for the SSRQs $\chi_v^2 \simeq 1.1$ for 5 degrees of freedom is obtained. That is, good fits to the luminosity functions are still obtained if the extreme values of R differ by factors of a few from what is observed.

3. p .—The value of p depends on the physics of the jets and the value we used, $p = 3 + \alpha$, is by no means the only choice. If we take $p = 2 + \alpha$, a good fit to the observed FSRQ luminosity function requires a value for R_{\max} smaller by a factor of 2–3 or a value of γ_2 larger by about the same factor. For example, if $R_{\max} = 500$ and we keep unchanged the other parameters, we obtain $\chi_v^2 \simeq 1.7$ for 4 degrees of freedom for the FSRQs ($p = 1.9$) and $\chi_v^2 \simeq 1.3$ for 5 degrees of freedom for the SSRQs ($p = 2.8$).

4. H_0 .—A change in the Hubble constant will affect the predicted and observed luminosity functions in the same way and so will not change the comparison between the beaming model and the data. However, the apparent velocities derived from superluminal data are inversely proportional to the Hubble constant. If $H_0 = 100 \text{ km s}^{-1} \text{ Mpc}^{-1}$, then $\gamma_1 = 2.5$ and $\gamma_2 = 20$. In this case both the FSRQ and SSRQ observed luminosity functions are not inconsistent with the predicted ones for $n(\gamma) \propto \gamma^{-3.8}$ (i.e., $\langle \gamma \rangle \simeq 3.8$), with $\chi_v^2 \simeq 2$ for 4 degrees of freedom and $\chi_v^2 \simeq 2$ for 5 degrees of freedom for FSRQs and SSRQs, respectively.

This analysis shows that, while the details of our model could change with better determined input parameters, the main result, i.e., the agreement between predicted and observed luminosity functions, is quite robust. Since the shape of the

luminosity function is affected by beaming, the comparison of luminosity functions is a strong test of the beaming hypothesis.

6.2. Predictions of the Model

The beaming model makes specific predictions for the luminosity functions of FSRQs and SSRQs below the limits of the 2 Jy catalog. For example, the FSRQs should have $\phi(P) \propto P_{2.7}^{-1.8}$ for $P \lesssim 3 \times 10^{33} \text{ ergs s}^{-1} \text{ Hz}^{-1}$. This should be easily testable when the optical identifications and redshift determinations of deeper radio samples are completed (e.g., Dunlop & Peacock 1990). The differential number counts predicted by our model for FSRQs and SSRQs are shown in Figure 5, which includes the 1σ uncertainty on τ . The fit was optimized for FSRQs so the best-fit differential counts of SSRQs are slightly below the data, but not significantly so.

Given the intrinsic range of Lorentz factors inferred for FSRQs and the range of angles derived by our model for SSRQs and F-R II galaxies, we can also predict the range of superluminal motion speeds for the latter classes. SSRQs should have $2.5 \lesssim \beta_{\text{app}} \lesssim 8.5$ while F-R II galaxies should have $\beta_{\text{app}} \lesssim 2.5$ ($H_0 = 50$). In this case, since the angles involved are larger than $\arcsin(1/\gamma_1) \simeq 11^\circ$, the distribution of β_{app} should be peaked at low values. This does not contradict the few data available for SSRQs: superluminal motion is observed in only one 2 Jy SSRQ, 3C 245, which has $\beta_{\text{app}} \sim 8$. The only other SSRQs with multiple epoch VLBI data, to our knowledge, are 3C 263 (Zensus, Hough, & Porcas 1987), which has $\beta_{\text{app}} \sim 3$ and 4C 34.47 (Barthel et al. 1989), which has $\beta_{\text{app}} \sim 5$. We note that 3C 245 has $\alpha = 0.57$ in Wall & Peacock 1985, but $\alpha = 0.51$ in the Parkes catalog (1990) and it is intermediate between lobe-dominated and core-dominated objects (Hough & Readhead 1987), although it is not an HPQ (Moore & Stockman 1984), so it could be a transitional object.

6.3. FSRQs as Beamed SSRQs?

For completeness, we also tested the idea that SSRQs are the parent population of FSRQs; with radio galaxies belonging to a separate class (Orr & Browne 1982). Contrary to the previous

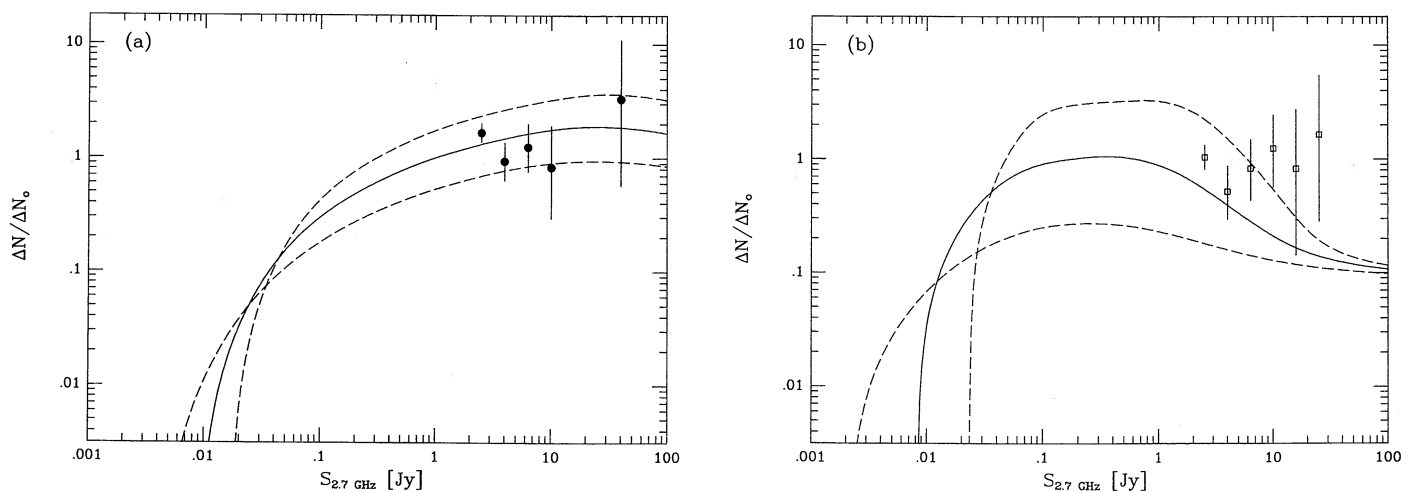


FIG. 5.—(a) The differential number counts for FSRQs normalized to Euclidean counts $\Delta N_0 = 17(S/\text{Jy})^{-2.5} \text{ Jy}^{-1} \text{ sr}^{-1}$. The solid line represents the prediction of our model, assuming $z_{\text{max}} = 3$, with the dashed lines indicating the range corresponding to a 1σ uncertainty on the evolutionary parameter τ . The 2 Jy FSRQs are also shown (filled circles). The error bars indicate 1σ errors assuming Poisson statistics (Gehrels 1986). (b) The differential number counts for SSRQs normalized as in (a). Note that the model parameters were fitted to the luminosity function of FSRQs and then they were shown to give a good fit to the one of SSRQs as well. A compromise fit to the luminosity functions of both FSRQs and SSRQs would improve the agreement between the predicted and observed counts.

picture, where F-R II galaxies were assumed to be the parents of both FSRQs and SSRQs, it proved quite difficult to fit the data. The shape of the predicted luminosity function was consistent with the observed one but the normalization was too low, i.e., there seem to be too few SSRQs for them to be the parents of FSRQs. The normalization can be increased by increasing f which means either increasing R_{\max} and/or diminishing γ_2 . A reasonable fit ($\chi^2_{\nu} \simeq 1.6$ for 4 degrees of freedom) to the observed luminosity function of FSRQs was obtained for a value of R_{\max} a factor of 5 higher than currently observed or a value of $\gamma_2 \simeq 20$, too low to be consistent with the superluminal data unless $H_0 = 100 \text{ km s}^{-1} \text{ Mpc}^{-1}$. This model predicts a range of observed superluminal motion speeds different from the previous one: in this case in fact FSRQs have $\theta \lesssim 15^\circ\text{--}17^\circ$, while SSRQs should go all the way up to $\theta \simeq 90^\circ$. Therefore, SSRQs should have $1 \lesssim \beta_{\text{app}} \lesssim 7$ (to be compared with $2.5 \lesssim \beta_{\text{app}} \lesssim 8.5$).

7. CONCLUSIONS

We have investigated the hypothesis that radio quasars are F-R II radio galaxies dominated by beamed emission from a relativistic jet. In this picture the angle of the jet to the line of sight should be small for flat-spectrum quasars, larger for steep-spectrum quasars, and still larger (up to 90°) for F-R II galaxies, while the intrinsic Lorentz factor(s) have to be the same. Our approach compares predicted and observed luminosity functions to test the model and constrain the few free parameters. To make this comparison, we first derived the local luminosity functions at 2.7 GHz for the various classes of radio sources.

Our main results are as follows.

1. We estimated the evolution of FSRQs, SSRQs, and F-R II

radio galaxies. We then derived their local luminosity functions, which are well represented by double power laws.

2. Superluminal data for FSRQs suggest a distribution of Lorentz factors $5 \lesssim \gamma \lesssim 40$. Good agreement between the predictions of a beaming model and the observed luminosity function of FSRQs was obtained for $n(\gamma) \propto \gamma^{-2.3}$, i.e., $\langle \gamma \rangle \simeq 11$. FSRQs should be aligned with the line of sight within $\sim 14^\circ$ ($\langle \theta \rangle \simeq 9^\circ$). The fraction of luminosity intrinsic to the jet is $\sim 1\%$.

3. Using the same intrinsic distribution of Lorentz factors the predicted luminosity function for SSRQs agrees well with the observed one. In this case we find $14^\circ \lesssim \theta \lesssim 40^\circ$ ($\langle \theta \rangle \simeq 28^\circ$). Although the best-fit solution could change with improved input data, the agreement between predictions and observations seems quite robust both for FSRQs and SSRQs.

4. The idea that FSRQs are beamed SSRQs (with F-R II galaxies belonging to a separate class) does not seem to fit the data as well, since it works only for a narrow range of input parameters. There seem to be too few SSRQs for them to constitute the parent population. The observed distribution of superluminal speeds for SSRQs should provide an additional constraint to this hypothesis.

In summary, we have demonstrated that the beaming hypothesis connecting radio galaxies and quasars is alive and well, providing that Lorentz factors of order 10 and jet luminosities of order 1% of the unbeamed luminosity are reasonable. Both superluminal motion data and observed ratios of beamed to unbeamed luminosity will provide further tests of our model.

We thank Manfred Stickel for providing the latest version of the 1 Jy catalog. This work was completed under the auspices of the STScI Visitor Program.

REFERENCES

- Antonucci, R. R. J., Hickson, P., Olszewski, E. W., & Miller, J. S. 1986, *AJ*, 92, 1
 Antonucci, R. R. J., & Ulvestad, J. S. 1985, *ApJ*, 294, 158
 Barthel, P. D. 1989, *ApJ*, 336, 606
 Barthel, P. D., Hooimeyer, J. R., Schilizzi, R. T., Miley, G. K., & Preuss, E. 1989, *ApJ*, 336, 601
 Blandford, R., & Rees, M. J. 1978, in *Pittsburgh Conference on BL Lac Objects*, ed. A. N. Wolfe (Pittsburgh: Univ. of Pittsburgh Press), 328
 Bridle, A. H., & Perley, R. A. 1984, *ARA&A*, 22, 319
 Browne, I. W. A. 1983, *MNRAS*, 204, 23P
 ———. 1989, in *BL Lac Objects*, ed. L. Maraschi, T. Maccacaro, & M.-H. Ulrich (New York: Springer), 401
 Browne, I. W. A., & Murphy, D. W. 1987, *MNRAS*, 226, 601
 Browne, I. W. A., & Perley, R. A. 1986, *MNRAS*, 222, 149
 Cawthorne, T. V. 1991, in *Beams and Jets in Astrophysics*, ed. P. A. Hughes (Cambridge: Cambridge Univ. Press), 187
 Cohen, M. H. 1989, in *BL Lac Objects*, ed. L. Maraschi, T. Maccacaro, & M.-H. Ulrich (New York: Springer), 13
 Danese, L., De Zotti, G., Franceschini, A., & Toffolatti, L. 1987, *ApJ*, 318, L15
 Djorgovski, S., Spinrad, H., McCarthy, P., Dickinson, M., van Bruegel, W., & Strom, R. G. 1988, *AJ*, 96, 836
 Dunlop, J. S., & Peacock, J. A. 1990, *MNRAS*, 247, 19
 Fanaroff, B. L., & Riley, J. M. 1974, *MNRAS*, 167, 31P
 Fugmann, W. 1988, *A&A*, 205, 86
 Gehrels, N. 1986, *ApJ*, 303, 336
 Hough, D. H., & Readhead, A. C. S. 1987, *ApJ*, 321, L11
 ———. 1989, *AJ*, 98, 1208
 Impey, C. D., Lawrence, C. R., & Tapia, S. 1991, *ApJ*, 375, 46
 Impey, C. D., & Tapia, S. 1990, *ApJ*, 354, 124
 Kellermann, K. I., Pauliny-Toth, I. I. K., & Williams, P. J. S. 1969, *ApJ*, 157, 1
 Kühr, H., Witzel, A., Pauliny-Toth, I. I. K., & Nauber, U. 1981, *A&AS*, 45, 367
 Laing, R. A., Riley, J. M., & Longair, M. S. 1983, *MNRAS*, 204, 151
 Lampton, M., Margon, B., & Bowyer, S. 1976, *ApJ*, 208, 177
 Lind, K. R., & Blandford, R. D. 1985, *ApJ*, 295, 358
 Longair, M. S., & Scheuer, P. A. G. 1970, *MNRAS*, 151, 45
 Maccacaro, T., Avni, I., Gioia, I. M., Giommi, P., Griffiths, R., Liebert, J., Stock, J. T., & Danziger, J. 1983, *ApJ*, 266, L73
 Marscher, A. P., Marshall, F. E., Mushotzky, R. F., Dent, W. A., Balonek, T. J., & Hartman, M. F. 1979, *ApJ*, 233, 498
 Moore, R. L., & Stockman, H. S. 1984, *ApJ*, 279, 465
 Mutel, R. L. 1990, in *Parsec-Scale Radio Jets*, ed. J. A. Zensus, & T. J. Pearson (Cambridge: Cambridge Univ. Press), 98
 Orr, M. J. L., & Browne, I. W. A. 1982, *MNRAS*, 200, 1067
 Padovani, P., & Urry, C. M. 1990, *ApJ*, 356, 75
 ———. 1991, *ApJ*, 368, 373
 Parkes Catalogue 1990, Australia Telescope National Facility
 Peacock, J. A. 1987, in *Astrophysical Jets and Their Engines*, ed. W. Kundt (Dordrecht: Reidel), 185
 Pearson, T. J., & Zensus, J. A. 1987, in *Superluminal Radio Sources*, ed. J. A. Zensus & T. J. Pearson (Cambridge: Cambridge Univ. Press), 1
 Porcas, R. W. 1987, in *Superluminal Radio Sources*, ed. J. A. Zensus & T. J. Pearson (Cambridge: Cambridge Univ. Press), 12
 Quirrenbach, A., Witzel, A., Krichbaum, T., Hummel, C. A., Alberdi, A., & Schalinski, C. 1989, *Nature*, 337, 442
 Scheuer, P. A. G., & Readhead, A. C. S. 1979, *Nature*, 277, 182
 Schmidt, M. 1968, *ApJ*, 151, 393
 Schwartz, D. A., & Ku, W. H.-M. 1983, *ApJ*, 266, 459
 Spinrad, H., Djorgovski, S., Marr, J., & Aguilar, L. 1985, *PASP*, 97, 932
 Stickel, M., & Kühr, H. 1992, in preparation
 Stickel, M., Padovani, P., Urry, C. M., Fried, J. W., & Kühr, H. 1991, *ApJ*, 374, 431
 Ulrich, M.-H. 1989, in *BL Lac Objects*, ed. L. Maraschi, T. Maccacaro, & M.-H. Ulrich (New York: Springer), 45
 Urry, C. M., & Padovani, P. 1991, *ApJ*, 371, 60
 Urry, C. M., Padovani, P., & Stickel, M. 1991, *ApJ*, 382, 501
 Urry, C. M., & Shafer, R. A. 1984, *ApJ*, 280, 569
 Véron-Cetty, M.-P., & Véron, P. 1989, *ESO Sci. Rep. No. 7*
 Wall, J. V., & Peacock, J. A. 1985, *MNRAS*, 216, 173
 Wardle, J. F. C., Moore, R. L., & Angel, J. R. P. 1984, *ApJ*, 279, 93
 Wehrle, A. E., Cohen, M. H., & Unwin, S. C. 1990, in *Parsec-Scale Radio Jets*, ed. J. A. Zensus & T. J. Pearson (Cambridge: Cambridge Univ. Press), 49
 Wills, B. J. 1989, in *BL Lac Objects*, ed. L. Maraschi, T. Maccacaro, & M.-H. Ulrich (New York: Springer), 109
 Wills, B. J., & Browne, I. W. A. 1986, *ApJ*, 302, 56
 Zensus, J. A. 1989, in *BL Lac Objects*, ed. L. Maraschi, T. Maccacaro, & M.-H. Ulrich (New York: Springer), 3
 Zensus, J. A., Hough, D. H., & Porcas, R. W. 1987, *Nature*, 325, 36